Comparative study on catalytic and non-catalytic pyrolysis of olive mill solid wastes

Comparative study on catalytic and non-catalytic pyrolysis of olive mill solid wastes

Elias A. Christoforou[a], Paris A. Fokaides[1a], Scott W. Banks[b], Daniel Nowakowski[b], Anthony V. Bridgwater[b], Stelios Stefanidis[c,d], Kostas G. Kalogiannis[c], Eleni F. Iliopoulou[c], Angelos A. Lappas[c]

[a] Sustainable Energy Research Group in Frederick University and Frederick Research Center, 7, Y. Frederickou Str., 1036, Nicosia, Cyprus

[b] Bioenergy Research Group, European Bioenergy Research Institute (EBRI), Aston University, Birmingham B4 7ET, United Kingdom

[c] Center of Research and Technology Hellas (CERTH), 6th km Charilaou-Thermi Rd, GR 57001 Thermi, Thessaloniki, Greece

[d] Department of Mechanical Engineering, University of Western Macedonia, Mpakola and Sialvera Str., 50100 Kozani, Greece

Abstract

In this study, catalytic and non-catalytic fast pyrolysis of dried olive husk and olive kernels was carried out. A bubbling fluidised bed reactor was used for the non-catalytic processing of the solid olive wastes. In-situ catalytic upgrading of biomass fast pyrolysis vapours was performed in a fixed bed bench-scale reactor at 500 °C, for catalyst screening purposes.

A maximum bio-oil yield of 47.35 wt.% (on dry biomass) was obtained from non-catalytic fast pyrolysis at a reaction temperature of 450 °C, while the bio-oil yield was decreased at 37.14 wt.% when the temperature was increased to 500 °C. In the case of the fixed bed unit tests, the highest liquid (52.66 wt.%) and organics (30.99 wt.%) yield was achieved with the use of the non-catalytic silica sand. Depending on the catalytic material, the liquid yield ranged from 47.03 wt.% to 43.96 wt.% the organic yield from 21.15 wt.% to 16.34 wt.% on dry biomass. Solid products were increased from 28.23 wt.% for the non-catalytic run to 32.81 wt.% on dry biomass, when MgO (5% Co) was used.

Keywords: olive husk, olive kernel, fast pyrolysis, catalytic pyrolysis, bio-oil, olive

1. Introduction

1.1 Olive mill solid wastes

The olive oil industry produces significant amounts of solid olive waste and their management and disposal remain an environmental challenge for olive mill operators. Olive husk, the solid

---

[1] Corresponding Author
Email address: eng.fp@frederick.ac.cy (P.A. Fokaides)

34 fraction derived from the olive oil extraction process using three-phase centrifugation, is a mixture

35 of olive kernels, pulp and skin. This residue, presents interesting thermochemical characteristics

36 which allow its exploitation for the production of clean energy. Pyrolysis is one of the most applied

37 thermochemical conversion methods for the utilisation of solid biomass resources and is an

38 effective and widely applied method for the conversion of solid olive mill wastes into useful

39 energy. The global olive production in 2013 exceeded 20 million tons. The Mediterranean region

40 accounted for more than 97% of the world total olive production with Spain, Italy and Greece

41 being the largest producers of olive oil (FAO, 2015).

42 The olive oil industry produces significant quantities of wastes, both solid and liquid, during the

43 oil extraction process. In the case of solid olive mill wastes, the produced amount of this residue

44 is significantly affected by the olive oil extraction method used. Three main technologies exist for

45 the extraction of olive oil namely pressing, three-phase and two-phase centrifugation. The

46 pressing method was widely used in the past for many centuries, while in the last decades, three

47 phase and two-phase centrifugation are the most widely applied technologies in olive mills (FAO,

48 2015, Roig et al. 2006). Although the amount of produced olive oil is similar between the

49 aforementioned centrifugal technologies, the amount and composition of the produced residues

50 significantly differs (Arvanitoyiannis and Kassaveti 2008).

51 The three-phase centrifugation system generates two waste streams; a solid residue called olive

52 husk or three-phase olive pomace (3POMW), which is a mixture of olive kernels, skin and pulp

53 and liquid fractions and the olive mill wastewaters (OMWW). On the other hand, the two-phase

54 centrifugation system produces a single waste stream, which is a solid/liquid mixture (2POMW)

55 residue also called two-phase olive pomace (Fokaides and Polycarpou, 2013, Christoforou and

56 Fokaides 2016, Niaounakis and Halvadakis 2004). The solid residue derived from the olive oil

57 production, is classified as a chemically untreated fruit residue, according to ISO 17225-1:2014.

58 Its thermochemical characteristics allow the potential exploitation of this solid residue for the

59 production of clean energy.

60 To this end, two main conversion pathways exist regarding the conversion of biomass to useful

61 energy, namely thermochemical and bio-chemical. Focused on the thermochemical conversion

62 of biomass to energy, different technologies exist for the conversion of biomass into useful forms

63 of energy (Christoforou and Fokaides 2016, Niaounakis and Halvadakis 2004, Encinar et al. 1996

64 .Caputo et al. 2003). In literature, pyrolysis has gained significant interest for the utilisation of

65 olive mill residues.

66

67 **1.2 Pyrolysis processing**

68 During pyrolysis the feedstock is decomposed in the absence of oxygen. The products of

69 pyrolysis are gases, liquids and solids and the obtained product yields depend on the applied

70 experimental conditions such as the reaction temperature, heating rate and hot vapour residence

71 time. The pyrolysis process can be slow or fast depending on the operating conditions. Biomass

72 fast pyrolysis requires rapid heating and relatively high reaction temperatures. Generally, high

73 temperatures and long hot vapour residence times result in higher gas yield while moderate

74 temperatures, high heat transfer rates and short hot vapour residence times are optimum for

75 producing liquids (Kendry 2002, Bridgwater 2012).

76 Catalytic pyrolysis regards the pyrolysis processing of biomass in the presence of catalyst, which,

77 depending on the operating conditions, results in cracking reactions and upgrading of biomass

78 pyrolysis products. The type of catalyst used in the reaction as well as the reactor configuration

79 play an important role in the production of primary products during pyrolysis. In the presence of

80 different catalysts, the primary pyrolysis vapours can be cracked to give liquid and gaseous fuels

81 (Sharma et al. 2015). The catalytic fast pyrolysis process may be either ex-situ or in-situ. In the

82 first method, the catalyst is incorporated in a separate reactor. In the second method, the catalyst

83 is mixed with the processed feedstock or placed within the same pyrolysis reactor (Galadima and

84 Muraza 2015).

85 Based on dry feedstock, the non catalytic thermal pyrolysis product yields are within the range

86 of 40–60 wt.% for organic condensates, 10–30 wt.% for gaseous products, 0–20 wt.% of solid

87 fraction (char), and 5-15 wt.% water (Uslu et al. 2008).

88

89 **1.3 Solid olive mill wastes pyrolysis**

90 Fast pyrolysis of solid olive mill wastes has been extensively studied in previously published

91 works. Şensöz et al. (2006) carried out pyrolysis of olive residues in a fixed-bed reactor and

92 investigated the effect of pyrolysis temperature, heating rate, particle size and sweep gas flow

93 rates on the pyrolysis product yields. The results indicated that both the temperature and heating

94 rate had a significant effect on the product yields. A maximum liquid yield of 37.7 wt.% was

95 achieved at the temperature of 500 °C, by applying a heating rate of 10 °C min.$^{-1}$ and a nitrogen

96 flow rate of 150 cm^3 min^{-1}. A feedstock with a particle size of 0.425–0.60 mm was used.

97 In another study of Putun et al. (2005)**Error! Reference source not found.**, pyrolysis of olive

98 residues has been conducted in a fixed bed reactor under various temperatures (400-700 °C),

99 gas flow rates (50-200 cm^3 min^{-1}) and steam velocities (0.6-2.7 cm s^{-1}). The results agreed with

100 the findings in Şensöz et al. (2006) since higher liquid production was obtained at 500 °C. Also,

101   a significant increase on the liquid product yield was observed for the experiment under nitrogen

102   and steam conditions compared with the static atmosphere. Zanzi et al. (2003) carried out fast

103   pyrolysis of olive waste and wheat straw at high temperatures (800–1000 °C). Higher char yields

104   were observed using olive wastes compared to wheat straw, due to the increased lignin content

105   of the feedstock. By increasing temperature, a reduction of the bio-char yield and an increase in

106   gaseous products was observed. A decrease of the CO_2 content in the gases and an increase

107   of the CO content for the agricultural residues was also observed.

108   Olive kernels (and cuttings) were pyrolysed in a captive sample reactor (wire mesh) by

109   Zabaniotou et al. (2000) in order to investigate the effect of pyrolysis temperature on the pyrolysis

110   product yields and composition. An increase in the gaseous yield was observed with increasing

111   temperature while CO, CO_2 and CH_4 were indicated as the dominant gas constituents. A

112   maximum bio-oil yield of 35 wt.% on dry basis was obtained at the temperature range of 450-550

113   °C, while the char yield reached 35 wt.%.

114   The pyrolysis of olive kernels has been investigated by Blanco Lopez et al. (2002) in order to

115   examine the effect of temperature, residence time and moisture content of the feedstock on the

116   pyrolysis product yields and quality of bio-oil. As in Zabaniotou et al. (2000), CO, CO_2 and CH_4

117   were found as the main gas components. The results of the study indicated an increase in the

118   aqueous fraction of liquid products, which was attributed to the larger extent of lignin

119   decomposition reactions. On the other hand, an increase in the non-aqueous fraction of liquid

120   products was observed with increasing residence time, which favors secondary reactions.

121   Finally, a decrease in the aqueous fraction was observed when feedstock with lower moisture

122   content was processed. Regarding energy content determination, the liquid products were found

123   to have the highest heating value.

124   Catalytic pyrolysis of solid olive mill wastes has also been investigated in many previously

125   published studies. Catalytic pyrolysis of olive husks and their conversion into hydrogen rich

126   gaseous products was examined by Caglar and Demirbas (2002) using $ZnCl_2$, Na_2CO_3, and

127   K_2CO_3 as catalysts in the study. The effect of temperature, space time, catalyst (calcined

128   dolomites) and steam on the elimination of tar in exhausted olive oil husks pyrolysis gas was

129   investigated by Taralas and Kontominas (2006). . The results indicated that an increase of the

130   temperature in non-catalytic runs diminishes the total tar content. Also, the presence of calcined

131   dolomite as tar elimination catalyst in olive kernels catalytic pyrolysis experiments, has led to an

132   increase in the H_2 yield compared with the non-catalytic experiments.

133   Slow, fast and catalytic pyrolysis of lignocellulosic biomass, including olive kernels, was

134   conducted by Zabaniotou et al. (2008). A captive sample wire mesh reactor was used for fast

135 pyrolysis experiments and a fixed bed reactor for non-catalytic and catalytic pyrolysis. Focused

136 on olive kernels, the authors concluded that olive kernels are suitable for liquid bio-fuels and also

137 for carbon black production via catalytic pyrolysis in a fixed bed reactor.

138 Encinar et al. (2008, 2009) carried out catalytic pyrolysis of olive oil waste using dolomite as

139 catalyst, aiming to characterise the char, tar and gases obtained in the pyrolysis process. The

140 utilisation of Encinar et al. (2009) dolomite activated as catalyst caused a decrease in the liquid

141 phase and an increase in the gas phase yield. When the mass of catalyst was increased, an

142 important decrease in the tar yield and a high increase in the gas phase yield were also observed.

143 In the study conducted by Demiral and Şensöz (2008), catalytic pyrolysis of olive and hazelnut

144 bagasse biomass samples was carried out in a fixed-bed reactor using activated alumina and

145 sodium feldspar as catalysts. The study aimed to investigate the effects of the catalysts and their

146 biomass to catalyst ratio on the pyrolysis product yields. The results were compared with non

147 catalytic experiments performed under the same conditions. With regard to olive bagasse, a

148 maximum bio-oil yield of 37.07 wt.% and 36.67 wt.% was obtained using activated alumina and

149 sodium feldspar as catalysts, respectively. A reduction of the oxygen content of bio-oils was

150 observed while the yield of bio-oil was reduced by the use of the catalysts.

151 The use of catalytic pyrolysis with ZSM-5, CaO and MgO catalysts is also a subject of interest

152 for many studies in the literature (Carlson et al., 2008, Zhang et al., 2009, Wang et al., 2010, Zhang et

153 al., 2013, Zhang et al., 2014).

154 The present work aimed to examine the thermal performance and properties of olive husk/kernels

155 and to evaluate its potential exploitation as a renewable feedstock for the production of fuels and

156 chemicals. Non-catalytic, fast pyrolysis of three-phase olive husk and olive kernels samples

157 aimed to investigate the effect of reaction temperature (i.e. 450, 500, 550 °C) and feedstock

158 composition on the pyrolysis product yields and the quality of the liquid products (i.e. bio-oil). The

159 experiments were carried out in a bubbling fluidized bed (BFB) reactor with a maximum feed

160 capacity of 1 kg h.$^{-1}$. In-situ catalytic upgrading of biomass fast pyrolysis vapours was performed

161 in a fixed bed bench-scale reactor at 500 °C, for catalyst screening purposes. Different catalysts

162 were used in the process and the obtained pyrolysis product yields as well as the composition of

163 those products were investigated. This is the first study in which fast pyrolysis is comparatively

164 assessed with catalytic pyrolysis for olive husk/kernels.

165

2. Material and methods

2.1 Biomass

Three-phase olive husk (TPOH) samples were collected from an olive mill located in Agglisides, Larnaca, Cyprus. The wet raw biomass was initially air-dried for a period of 10 h at 105 °C in a SNOL 20-300 electric furnace and packaged in air-tight bags.

2.2 Catalysts

Silica sand was used for the thermal pyrolysis tests, while an industrial ZSM-5 catalyst in microsphere formulation was used for the in situ upgrading tests. The silica sand had a particle size distribution between 60 and 300 μm and a mean particle size of 134.5 μm. The ZSM-5 catalyst is a typical commercial ZSM-5. The ZSM-5 zeolite was supported on silica alumina, with a SiO_2/Al_2O_3 ratio of about 20. The zeolite weight percentage in the catalyst was 30 wt.% and the total surface area was 140 m^2 g^{-1}. This catalyst has been studied before by our group in biomass pyrolysis upgrading and has been found to efficiently deoxygenate biomass pyrolysis vapors. Additionally, as an industrial ZSM-5 catalyst, it can provide insight in how this system would actually behave in a commercial process. The catalyst acidity was evaluated by FTIR analysis with pyridine adsorption and revealed a Brønsted, Lewis and total acidity of the catalyst of 45.9, 4.9 and 50.8 μmol/g respectively. A Co-impregnated sample of the same ZSM-5 catalyst was also tested. This catalyst sample was produced via a typical wet impregnation method using an aqueous solution of $Co(NO_3)_2.6H_2O$ salt. Details have been described elsewhere (Iliopoulou et al. 2012). The Co-ZSM-5 catalyst had a surface area of 158 m^2 g^{-1} and Brønsted, Lewis and total acidity of 28.8, 133.0 and 161.8 μmol g^{-1} respectively.

The MgO material used had a surface area of 64 m^2 g^{-1}. Its average pore diameter was 28.9 nm and its total pore volume was 0.36 cm^3 g^{-1}. The basicity of the MgO material was measured by temperature programmed desorption of CO_2 and was found to be 244 μmol CO_2 g^{-1}. The acidity of the material was not measured but it is expected to be negligible. The Co-MgO catalyst was prepared in a similar way as the Co-ZSM-5 catalyst. The Co- doped MgO had a reduced surface area of 46 m^2 g^{-1}. Its average pore diameter was 37.0 nm and its total pore volume was 0.43 cm^3 g^{-1} (Deng et al. 2006, Gaertner et al. 2009, Mante et al. 2015, Snell et al. 2010). Prior to the experiments, the catalytic materials were calcined at 500 °C for 3 h and stored in a desiccator. The choice of the catalysts was done in order to satisfy both acid and base catalysis conditions.

198 **2.3 Raw material preparation and characterization**

199 2.3.1   Sample preparation

200 In order to ensure homogeneity, prior to non-catalytic fast pyrolysis processing the sample was

201 milled using a Retsch, SM 2000 cutting mill. The sample was then sieved in an Endecotts

202 Powermatic Sieve Shaker to obtain particle size fraction of 0.25-2.00 mm for the fast pyrolysis

203 processing. Sub-samples which consisted mainly of olive kernels (after the removal of olive pulp

204 and skin) were also prepared for experimental analysis.

205

206 2.3.2   Moisture and ash content determination

207 Moisture content determination of the sample was carried out using an MA 35, Santorius

208 moisture analyzer. The ash content of the feedstock and bio-char was determined according to

209 E 1755 ASTM method, using a Carbolite AAF1100 furnace.

210

211 2.3.3   Elemental analysis and Calorific value determination

212 The determination of the carbon, hydrogen and nitrogen content (wt.% on dry basis) was done

213 using a Carlo-Erba, EA 1108 elemental analyser. The results reported were the average result

214 obtained from two replications. The gross calorific value of the samples were calculated

215 according to Eqs. (1) (Christoforou et al. 2014) and (2) (Yin 2011), using carbon, hydrogen and

216 nitrogen concentrations and an average value was taken.

$$\mathrm{HHV_{dry}} = 987.1628 C^{0.7587} + 683.0607 H^{0.3645} + 105.5334 N^{3.2688} \qquad (1)$$
$$+ \ 862.0001$$

$$\mathrm{HHV_{dry}} = 0.2949\,C + 0.825 H \qquad (2)$$

217 The lower heating value (LHV) was calculated using Eq.(3) (ECN 2011):

$$\mathrm{LHV_{dry}} = \mathrm{HHV_{dry}} - 2.443 * 8.936 (H/100) \qquad (3)$$

218 **2.4 Non-catalytic BFB fast pyrolysis**

219 2.4.1   Experimental set -up

220 The pyrolysis experiments were carried out using a continuous bubbling fluidised bed reactor

221 with maximum feed flow of 1 kg hr.[-1] **(Fig. 1)**. Sieved quartz sand (1 kg) with a particle size

222 between 600 and 710 µm was used as the bed material and electrically pre-heated nitrogen was

223 used as the fluidising gas in the reactor. A single pass basis was used so that the gas stream

224 (nitrogen and product gas) could be analysed every 150 s. A constant biomass feed rate was

225 applied to the procedure using an air-tight hopper with a double screw feeder attached to a water

226 cooled fast screw. The char was separated from the gas and vapour stream by passing through

227 two heated cyclones in series. The condensation of vapours in a cooled quench column followed

228 using ISOPAR™ V as the quenching media, and the bio oil was finally collected in a collection

229 tank. The aerosols were coalesced in a wet walled electrostatic precipitator. Following the

230 electrostatic precipitator the gas passed through a water cooled condenser, two dry ice–acetone

231 condensers in series and finally a cotton wool filter, followed by 250 g of silica gel (Banks et al.

232 2014).

233 Olive husk was pyrolysed under three different pyrolysis temperatures; 450, 500, and 550 °C.

234 The duration of each experimental run was 90 minutes. In addition, a single run of olive kernels

235 pyrolysis was carried out at 500 °C and by applying slightly increased fluidising velocity, due to

236 which the duration of this run was reduced to 47 minutes.

237 **Figure 1**

238 2.4.2   Fast pyrolysis products analysis

239 Water content, class and dynamic viscosity of bio-oils

240 The water content of all the fast pyrolysis liquids was determined using a Mettler Toledo V20

241 Karl-Fischer (KF) titrator. Hydranal (R) K and Hydranal (R) Composite 5 K was used as the

242 working medium and titrant respectively. The KF titrator was calibrated with HPLC–grade water

243 prior to the analysis of the fast pyrolysis products. The experiments were performed in triplicate

244 and the water content was automatically calculated by the KF titrator, based on the weight of bio-

245 oil sample used. The class of bio-oil was defined by taking measurements from three separate

246 points of the bio-oil sample, from top to bottom. A single phase bio-oil is defined when the

247 difference between two consecutive points is lower than 1 wt.%, while it is defined as separated

248 when any one of the measurements falls outside of the 4 wt.% range (Banks et al. 2014).

249 The dynamic viscosity of bio-oil samples was carried out using a DV-II+ pro rotational viscometer

250 by Brookfield Viscometer. An increasing speed was used (0.5 rpm for 120 minutes) while the

251 initial speed was set to give a 10% torque. A temperature controlled water bath at 40 ±0.1 °C

252 was also used for the analysis.

253 The acidity of the bio oils was measured with a Sartorius PB-11 pH basic meter. Prior to the

254 measurement the pH meter was calibrated with pH buffers.

255 Gas chromatography–mass spectrometry (GC-MS) analysis of fast pyrolysis liquids

256 Varian GC-450 chromatograph and MS-220 mass spectrometer were used to analyse the

257 chemical composition of fast pyrolysis bio-oil. GC samples were prepared by mixing GC grade

258 acetone with bio-oil at a ratio of 3:1 (v v^{-1}). For each analysis 1 µl of GC sample was injected

259 onto the GC column, helium was used as the carrier gas and the mass spectra were obtained

260 for a molecular mass range (m/z) of 45 to 300. A Varian FactorFour® column was used (30 m,

261 0.25 mm id., 0.25 µm df) to separate bio-oil components. The injection port was kept at 250ᵒC

262 and a 1:75 split ratio was used. The GC oven was held at 45 °C for 2.5 minutes, then heated at

263 5 °C min.[-1] to 250 °C and held at this temperature for 7.5 minutes. Proposed peak assignments

264 (m/z = 45-300) were made from mass spectra detection using the NIST05 MS library and from

265 assignments in the literature (Faix 1990).

266 Gas chromatography analysis of fast pyrolysis gaseous products

267 An on-line Varian CP 4900 Micro-GC microgas chromatograph equipped with a thermal

268 conductivity detector and two columns was used for the analysis of the non-condensable gases

269 obtained from the fast pyrolysis experiments. Measurements were taken every 150s.

270

271 **2.5 In-situ catalytic pyrolysis**

272 2.5.1   Experimental set -up

273 All pyrolysis experiments were performed at 500 °C, using a bench-scale fixed bed reactor, made

274 of stainless steel 316 and heated by a 3-zone furnace. The temperature of each zone was

275 independently controlled using temperature controllers. The catalyst bed temperature was

276 considered as the experiment temperature and was monitored with a thermowell. A specially

277 designed piston system was used to introduce the biomass feedstock into the reactor. A constant

278 stream of N_2 was fed from the top of the reactor for the continuous withdrawal of the products

279 and in order to maintain an inert atmosphere during pyrolysis. The products exited from the

280 bottom of the reactor in gaseous form and were condensed in a glass receiver submerged in a

281 cooling bath kept at 17 °C. Non-condensable gases were collected in a gas collection system. A

282 filter placed between the glass receiver and the gas collection system recovered any

283 condensable gases that were not condensed in the receiver. A schematic diagram of the

284 experimental set-up is given in **Fig. 2**.

285   **Figure 2**

286

287 2.5.2   Experimental Procedure and Products Collection

288 Initially, the reactor was filled with 0.7 g catalyst or silica sand for the catalytic and non-catalytic

289 tests, respectively, and the piston was filled with 1.5 g of biomass. As soon as the desired

290 reaction tempera-ture was reached, the biomass was introduced into the reactor and the

291 experiment began using a 100 cm³ min.[-1] nitrogen flow. At the end of the experiment (15 min),

292 the reactor was cooled and purged for 10 min with N_2 (50 cm³ min.[-1]). For all tests the reactor

293 temperature was kept constant at 500 °C. The liquid products were collected and quantitatively

294 measured in the pre-weighted glass receiver. The pyrolytic vapours, upon their condensation in

295 the glass receiver, formed multiple phases; an aqueous phase, a liquid organic phase and

296 viscous organic deposits on the receiver walls.

297 In order to achieve the collection of a representative bio-oil sample for analysis, the bio-oil was

298 first fully homogenised inside the receiver using ethyl lactate as the solvent and then collected

299 as a solution, which was then submitted for analysis. The gas products were collected and

300 measured by the water displacement method. The amount of condensable vapours recovered in

301 the filter was also measured by direct weighing and was added to the liquid products yield. The

302 amount of the solid residue formed was measured by direct weighing. The solid products

303 consisted of charcoal (biomass residue) and coke-on-catalyst formed by thermal and catalytic

304 cracking, as well as a very small amount of unreacted biomass. Three experiments under the

305 same conditions were realised for each catalytic material in order to ensure repeatability and the

306 average values from the three experimental runs are reported.

307

308 2.5.3   Pyrolysis products analysis

309 The water content of the bio-oil was determined by Karl-Fischer titration (ASTM E203-08). The

310 water/aqueous phase present in the bio-oil was separated from the organic phase using an

311 organic solvent (dichloromethane) and the organic phase was analysed by GC-MS using an

312 Agilent 7890A/5975C gas chromatograph-mass spectrometer system (Electron energy 70 eV,

313 Emission 300 V, Helium flow rate: 0.7 cm^3 min.$^{-1}$, Column: HP-5MS 30 m x 0.25 mm ID x 0.25

314 µm). The NIST05 mass spectral library was used for the identification of the compounds found

315 in the bio-oil and internal libraries were used for their categorisation into main functional groups.

316 The non-condensable gases were analysed in a HP 5890 Series II gas chromatograph equipped

317 with four columns (Precolumn: OV-101, Columns: Porapak N, Molecular Sieve 5A and Rt-Qplot

318 30 m x 0.53 mm ID) and two detectors (TCD and FID).

319

320 **3.   Results and Discussion**

321 **3.1 Feedstock characterisation**

322 The results obtained from the elemental analysis of the processed feedstock are given in **Table**

323 **1**. According to the results, higher C, H and N values were determined for olive husks compared

324 to olive kernel sample, while the same trend was observed regarding the ash content

325 determination. Furthermore, olive husk presented higher moisture content (3.66%) compared to

326 olive kernel (1.53%). The LHV was calculated as 20.07 MJ kg^{-1} and 19.0 MJ kg^{-1} for olive husks

327 and kernel samples respectively.

328 **Table 1**

329

330 **3.2 Non-catalytic fast pyrolysis processing**

331 3.2.1   Product yields

332 **Table 2** presents the product yields obtained at pyrolysis temperatures of 450 °C, 500 °C and

333 550 °C for olive husks and 500 °C for olive kernels. As it can be seen, olive husk pyrolysis mass

334 balances closure was within the range of 76.29-87 wt.%, while acceptable mass balance of 91.63

335 wt.% was obtained from the olive kernels experimental run. This can be attributed to the high

336 ash content of the samples and the mixed nature of the feedstock which resulted in higher water

337 content losses in the system and subsequently lower mass balance closures.

338 A maximum bio-oil value of 47.35 wt.% was observed at a reaction temperature of 450 °C.

339 Decrease of bio-oil yield (37.14 wt.%) was observed with increasing temperature at 500 °C while

340 a slight increase in the liquid fraction (40.15 wt.%) was observed at 550 °C. Char yields

341 presented a similar trend with 24.69 wt.%, 21.25 wt.% and 21.33 wt.% at 450 °C, 500 °C and

342 550 °C respectively. Finally, the gas product yield increased with pyrolysis temperature reaching

343 a maximum value of 21.38 wt.% at the final temperature of 550 °C. The increase in gas products

344 is thought to occur predominantly due to secondary cracking of the pyrolysis vapours at higher

345 temperatures (Şensöz et al. 2006). Similar results regarding the yields of pyrolysis products in

346 the temperature range of 450-550 °C were found in previously published studies. Liquid yields

347 of 30.7-42.9 wt.%, gas yields of 13.5-20.1 wt.% and char within the range of 30.6-37 wt.% have

348 been reported in previous studies (Encinar et al. 1996, Şensöz et al. 2006, Pütün 2005,

349 Zabaniotou 2000).

350 **Table 2**

351 By comparing the product yields obtained from the pyrolysis of olive husk and kernels at 500 °C,

352 a higher bio-oil production (53.62 wt.%) was achieved with the pyrolysis of olive kernels while

353 char and gas production was slightly lower, 21.02 and 16.99 wt.% respectively. The reported

354 value of bio-oil yield is significantly higher compared to previously reported data in literature (i.e.

355 29 wt.%) (Zabaniotou et al. 2000) where olive kernel pyrolysis was investigated. Higher gaseous

356 and solid yields were also reported in Zabaniotou et al. (2000).

357

358 3.2.2   Gas analysis

359 **Fig. 3** presents the main components of the pyrolysis gases for the non-catalytic experimental

360 runs conducted within this study. CO_2, CO, CH_4 and C_3H_6 were identified as the major

361 components of the obtained gas mixture. Other minor components were C_2H_4, C_2H_6 and C_3H_8.

362 As it can be observed, the composition of the pyrolysis gas mixture depends on the reaction

363 temperature.

364 In contrast to previously published works where a decreased yield of CO_2 with increasing

365 temperature was reported (Lopez et al. 2002, Uzun et al. 2007), CO_2, CO and CH_4 presented an

366 increasing trend with increased temperature reaching a maximum value of 9.49%, 6.24% and

367 1.46% respectively at 550 °C. Propene yield presented similar trend with a slight decrease at the

368 temperature of 500 °C followed by a maximum concentration of 1.34% at 550 °C.

369 The release of CO and CO_2 could be due to the degradation of hemicellulose, and cellulose and

370 lignin (Lopez et al. 2002, Uzun et al. 2007). The increased formation of CH_4 and light

371 hydrocarbons and other light hydrocarbons at higher temperatures is more likely due to the

372 secondary cracking reactions of the primary volatiles from cellulose, hemicellulose and lignin.

373 Fig. 3 also presents the gas mixture composition obtained from the pyrolysis of olive kernels at

374 500 °C. By comparing the obtained results with those obtained from the pyrolysis of olive husk

375 at the same temperature (i.e. 500 °C), increased CO (4.95%) fraction can be observed while

376 CO_2 (8.01%) presents significant decrease. CH_4 (0.98%) and C_3H_6 (0.97%) were also slightly

377 reduced.

378 **Figure 3**

379 3.2.3 <u>Char analysis</u>

380 The results of proximal and elemental analysis of char are given in **Table 3**. As it can be observed

381 the ash content presents an average value of 15.44% at 450 °C, slightly decreases at 500 °C

382 (14.26%) and presents a significant increase and a maximum at 550 °C (35.1%). The high ash

383 content of char obtained at 550 °C could be attributed to sand attrition resulting in the sand

384 particle size decreasing and therefore becoming entrained out of the reactor bed with the char.

385 Char ash content values of 16.77 and 20.17 at 500 and 550 °C were reported in (Uzun et al.

386 2007), as obtained from fast pyrolysis of unspecified olive residues.

387 Regarding C, H and N content of char, similar results have been reported in previous studies

388 during pyrolysis of olive residues at the temperature of 500 °C. Specifically, carbon, hydrogen

389 and nitrogen content of char was found in the range of 56.21-73.1, 2.1-2.3 and 0.32-2.6

390 respectively (Şensöz et al. 2006, Pütün et al. 2005, Uzun et al. 2007)

391 **Table 3**

392 3.2.4 <u>Bio-oil characterisation</u>

393 **Table 4** present the results obtained from the elemental analysis of bio-oil samples.

394   As it can be observed, the viscosity of the organic phase of bio-oil samples derived from olive

395   husk pyrolysis was increased with temperature, whilst there was no significant difference in water

396   content which could possibly lead to increased viscosity. In contrast to the olive kernels run where

397   a single phase liquid product was obtained, separated liquid phases were retrieved from the

398   pyrolysis of olive husk samples in all temperatures.

399   <div align="center">**Table 4**</div>

400   Figure 4 presents the chromatograms obtained from the analysis of bio-oils using GC/MS. The

401   results of the chemical composition of the bio-oils as derived from GC-MS are given in Table 5.

402   It can be concluded that the bio-oil produced from olive husk at higher temperatures had lower

403   levels of phenols (24.6%) but had higher ketone levels (20.5%). An increased pyrolysis reaction

404   temperature from 450 °C to 550 °C resulted in an increase of undesirable compounds with acids

405   (2.8% and 5.7% respectively), aldehydes (2.0% and 2.6% respectively) and ketones (10.8% and

406   20.5% respectively) providing a bio-oil with a reduced stability. This can be attributed to more

407   intense cracking reactions occurring during fast pyrolysis. Bio-oil produced from olive kernels

408   after being separated from the three phase olive husk feed material had higher levels of phenols

409   (40.0%) and lower levels of ketones (8.9%) and acids (1.1%). The only undesirable compound

410   that showed increased levels was aldehydes (6.6%). An increase in desirable compounds and a

411   general reduction in undesirable compounds can be attributed to lower feed ash content (0.48

412   wt. %). As the feed has lower ash content the cracking reactions are reduced, leading to a better

413   stability bio-oil.

414   <div align="center">**Figure 4**</div>

415   <div align="center">**Table 5**</div>

416

417   **3.3 Catalytic pyrolysis processing and products characterisation**

418   3.3.1   <u>Product yields</u>

419   The liquid, gas, solid, water and organic product yields (wt.% based on biomass) obtained by the

420   in situ catalytic upgrading of olive husk and kernels pyrolysis products are given in Table 6. Each

421   catalytic material affected the product yields to a different extent. The highest liquid (52.66 wt.%)

422   and organics (30.99 wt.%) yield was achieved with the use of the non-catalytic silica sand.

423   Depending on the catalytic material, the liquid yield ranged from 47.03 wt.% to 43.96 wt.% on

424   dry biomass and the organic yield from 21.15 wt.% to 16.34 wt.% on dry biomass.

425   <div align="center">**Table 6**</div>

426   The solid products yield increased as well, ranging from 28.23 wt.% for the non-catalytic run to

427   32.81 wt.% on biomass, when using MgO (5% Co). The solid products include both the biomass

428   residue (char) and the catalytically produced coke on the pores of the catalyst. Since the biomass

429   and the catalyst bed are not in contact, the presence of the catalytic material does not affect the

430   decomposition of the solid biomass feed. Therefore, the char yield can be considered constant

431   for all catalysts. Higher solid product yields in the catalytic runs are tentatively attributed to coke

432   deposits on the catalyst formed from catalytically driven reactions.

433   The main gaseous products detected and measured were CO_2 and CO. CH_4 and H_2, as well as

434   other light hydrocarbons in significantly smaller quantities, mainly C_2– C_6 light hydrocarbons.

435   Table 7 presents CO_2, CO and other gas yields for each catalyst used. The MgO (5% Co) catalyst

436   led to a considerable increase in CO_2 yield of 15.79 wt.% on biomass. Catalytic runs led to

437   oxygen removal from the pyrolysis vapours in the form of CO_2, CO and H_2O. The removal of

438   oxygen in the form of CO_2 is the most preferable route because only one carbon atom is required

439   for the removal of two oxygen atoms, whereas in the case of CO formation, one carbon atom is

440   required for each oxygen atom that is removed. The increase in CO_2 production with the MgO

441   and the MgO (5% Co) catalysts was attributed to ketonisation and aldol condensation reactions

442   that are catalysed by the basic sites of the catalyst (Deng et al. 2009, Snell et al. 2010).

443   **Table 7**

444   In contrast it can be observed that the increase of total gas yield for acidic materials (ZSM-5,

445   ZSM-5 (5% Co)) is mainly due to the increase in the production of CO. CO production is mostly

446   attributed to decarbonylation reactions that are favored by the acid sites of the catalyst.

447

448   3.3.2   <u>Chemical Composition of the bio-oil</u>

449   Table 8 presents the qualitative composition results of the bio oil's organic fraction (from GC–MS

450   analysis). The identified compounds were classified into the following groups; aromatic

451   hydrocarbons (AR), aliphatic hydrocarbons (ALI), phenols (PH), acids (AC), alcohols (AL),

452   aldehydes (ALD), ketones (KET), polycyclic aromatic hydrocarbons (PAH) and other oxygenates

453   (OXY). The "other oxygenates" group includes compounds such as furans, esters and ethers.

454   Compounds with very high molecular weights that could not be analysed by the GC–MS system

455   were classified as heavy compounds (HV). The latter category of compounds appeared as a

456   large wide peak at the end of the chromatogram.

457   **Table 8**

458   In general the compounds can be classified into two groups, those considered as desirable and

459   those which are undesirable. In the first category belong aromatic hydrocarbons, aliphatic

460   hydrocarbons and alcohols. Also phenols and furans are high added value chemicals and high

461   yields of these compounds can help the process become more economically attractive. The

462 compounds which are considered as undesirable, especially for energy production purposes are

463 ketones, aldehydes and heavy compounds. These compounds are considered responsible for

464 the aging reactions in the bio-oil and greatly affect its quality. Also acids cause corrosion and

465 they are difficult to introduce into engines. They also catalyse polymerisation reactions,

466 decreasing in this manner the stability of the bio-oil. PAHs are considered carcinogenic and

467 therefore hazardous for the environment. Finally esters, ethers and in general oxygenates reduce

468 the heating value of the bio-oil.

469 It can be concluded from Table 8 that the bio-oil produced from non-catalytic pyrolysis had low

470 levels of phenols (2.9%) but had high acids (21.1%) and heavy compounds content (31.5%).

471 Some catalysts were very effective in reducing the undesirable compounds ZSM-5 (5%Co) and

472 MgO (5%Co) were effective in reducing heavy compound concentrations (14.2% and 24.7%

473 respectively) providing a bio-oil with better stability. ZSM-5 catalytic material was the most

474 selective towards aromatic hydrocarbons production (11.9%). On the downside ZSM-5's organic

475 fraction yield was low, (19.68 wt.%) on initial biomass. Cracking of the pyrolysis vapours led to

476 an increase of coke, gases and H_2O. Thus, the overall process efficiency was reduced in favour

477 of a better quality bio-oil, represented by its low oxygen content.

478

479 3.3.3   Elemental Composition of the organic fraction

480 Table 9 presents the elemental composition of the bio-oil's organic fraction as produced with

481 each catalyst. The organic fraction of the thermal pyrolysis bio-oil was highly oxygenated

482 (37.06% oxygen content). The oxygen content of the organic fraction was reduced with the use

483 of all catalytic materials. The most deoxygenated bio-oils were produced with the MgO (23.93%

484 oxygen content) catalyst, which also gave the highest liquid organic fraction yield. The good

485 performance of the MgO catalyst can be attributed to its selectivity towards removal of oxygen

486 via formation of CO_2 (from ketonisation and aldol condensation reactions, Table 7), which is the

487 most carbon efficient pathway for oxygen elimination and to the low affinity for coke formation,

488 evident by the relatively low solid product yields (Table 6).

489 **Table 9**

490

491 **4. Conclusions**

492 The study aimed to examine the thermal performance and properties of olive husk and olive

493 kernels and evaluate their potential exploitation as a renewable feedstock for the production of

494 fuels and chemicals through the employment of non-catalytic and catalytic fast pyrolysis.

Non-catalytic pyrolysis experiments were carried out in a BFB reactor at different reaction temperatures (i.e. 450, 500, 550 °C). Olive husk samples pyrolysis gave separated liquid phases in all temperatures, with a maximum bio-oil yield of 47.35% observed at 450 °C. In contrast to the olive husk processing, a single phase liquid product was obtained from olive kernels pyrolysis which also gave higher bio-oil yield of 53.62% at 500°C compared to the olive husk run at the same temperature. The viscosity of the organic phase of bio-oil samples derived from olive husk pyrolysis was found to increase with temperature.

The results of bio-oil characterisation derived from olive husk pyrolysis, indicated an increase of undesirable compounds with acids, aldehydes and ketones providing a bio-oil with a reduced stability with increased pyrolysis reaction temperature. Bio-oil produced from olive kernels had higher levels of phenols and lower levels of ketones. The in-situ upgrading of olive husk/kernels pyrolysis vapours over various catalytic materials was studied in a fixed bed pyrolysis reactor. The catalytic materials were evaluated with respect to organic liquid product yield, deoxygenation ability and selectivity towards desirable compounds. The highest liquid and organics yield was achieved with the use of the non-catalytic silica sand. The study indicated that the presence of the catalytic material does not affect the decomposition of the solid biomass feed. The use of all catalytic material was found to reduce the oxygen content of the organic fraction while the most deoxygenated bio-oils were produced with the use of MgO catalyst. The difference in the bio-oil yield between the catalytic and the non-catalytic process is due to the fact that catalytic cracking accomplishes deoxygenation through simultaneous dehydration, decarboxylation, and decarbonylation reactions occurring in the presence of catalysts, whereas fast pyrolysis conditions are most suitable rate to break the heat and mass transfer limitations.

The experimental investigation of olive husk/kernels and thus the results of this study are expected to have a significant impact on the development of the exploitation methods of solid wastes produced in the olive oil industry, especially in the Mediterranean basin. The results obtained from pyrolysis experiments as well as the characterisation of the products of pyrolysis reaction, will specify the potential contribution of this biomass resource, mixture of olive husk/olive kernels, to the production of bio oil. The potential of fine chemicals production besides biofuels will be further explored.

Acknowledgement

References

Arvanitoyannis, I. S., Kassaveti, A., & Stefanatos, S. (2007). Current and potential uses of thermally treated olive oil waste. International journal of food science & technology, 42(7), 852-867.

ASTM, Standard Test Method for ash in Biomass, ASTM International, West Conshohocken, PA, 2007

Banks, S. W., Nowakowski, D. J., & Bridgwater, A. V. (2014). Fast pyrolysis processing of surfactant washed Miscanthus. Fuel Processing Technology, 128, 94-103.

Bridgwater, A. V. (2012). Review of fast pyrolysis of biomass and product upgrading. Biomass and bioenergy, 38, 68-94.

Çağlar, A., & Demirbaş, A. (2002). Hydrogen rich gas mixture from olive husk via pyrolysis. Energy Conversion and Management, 43(1), 109-117.

Caputo, A. C., Scacchia, F., & Pelagagge, P. M. (2003). Disposal of by-products in olive oil industry: waste-to-energy solutions. Applied Thermal Engineering, 23(2), 197-214.

Carlson, T. R., Vispute, T. P., & Huber, G. W. (2008). Green gasoline by catalytic fast pyrolysis of solid biomass derived compounds. ChemSusChem, 1(5), 397-400.

Christoforou, E. A., Fokaides, P. A., & Kyriakides, I. (2014). Monte Carlo parametric modeling for predicting biomass calorific value. Journal of Thermal Analysis and Calorimetry, 118(3), 1789-1796.

Christoforou, E., & Fokaides, P. A. (2016). A review of olive mill solid wastes to energy utilization techniques. Waste Management, 49, 346-363.

Demiral, I., & Şensöz, S. (2008). The effects of different catalysts on the pyrolysis of industrial wastes (olive and hazelnut bagasse). Bioresource technology, 99(17), 8002-8007.

Deng, L., Fu, Y., & Guo, Q. X. (2009). Upgraded acidic components of bio-oil through catalytic ketonic condensation. Energy & Fuels, 23(1), 564-568.

ECN, Phyllis, database for biomass and waste, Energy research Centre of the Netherlands, in, Energy research Centre of the Netherlands, 2011.

Encinar, J. M., Beltran, F. J., Bernalte, A., Ramiro, A., & Gonzalez, J. F. (1996). Pyrolysis of two agricultural residues: olive and grape bagasse. Influence of particle size and temperature. Biomass and Bioenergy, 11(5), 397-409.

Encinar, J. M., González, J. F., Martínez, G., & González, J. M. (2008). Two stages catalytic pyrolysis of olive oil waste. Fuel Processing Technology, 89(12), 1448-1455.

Encinar, J. M., Gonzalez, J. F., Martinez, G., & Roman, S. (2009). Catalytic pyrolysis of exhausted olive oil waste. Journal of Analytical and Applied Pyrolysis, 85(1), 197-203.

Faix, O., Meier, D., & Fortmann, I. (1990). Thermal degradation products of wood. Holz als Roh-und Werkstoff, 48(7-8), 281-285.

Fokaides, P. A., & Polycarpou, P. (2013). Exploitation of olive solid waste for energy purposes. Renewable energy, economies, emerging technologies and global practices. New York: Nova Science Publishers, Inc, 163-78.

Food and Agriculture Organization of the United Nations - Statistics Division, http://faostat3.fao.org, last visited 02 December 2015.

Gaertner, C. A., Serrano-Ruiz, J. C., Braden, D. J., & Dumesic, J. A. (2009). Catalytic coupling of carboxylic acids by ketonization as a processing step in biomass conversion. Journal of Catalysis, 266(1), 71-78.

Galadima, A., & Muraza, O. (2015). In situ fast pyrolysis of biomass with zeolite catalysts for bioaromatics/gasoline production: A review. Energy Conversion and Management, 105, 338-354.

Iliopoulou, E. F., Stefanidis, S. D., Kalogiannis, K. G., Delimitis, A., Lappas, A. A., & Triantafyllidis, K. S. (2012). Catalytic upgrading of biomass pyrolysis vapors using transition metal-modified ZSM-5 zeolite. Applied Catalysis B: Environmental, 127, 281-290.

ISO 17225-1-2014, Solid biofuels - Fuel specifications and classes - Part 1: General requirements, 2014.

López, M. B., Blanco, C. G., Martınez-Alonso, A., & Tascón, J. M. D. (2002). Composition of gases released during olive stones pyrolysis. Journal of analytical and applied pyrolysis, 65(2), 313-322.

Mante, O. D., Rodriguez, J. A., Senanayake, S. D., & Babu, S. P. (2015). Catalytic conversion of biomass pyrolysis vapors into hydrocarbon fuel precursors. Green Chemistry, 17(4), 2362-2368.

McKendry, P. (2002). Energy production from biomass (part 2): conversion technologies. Bioresource technology, 83(1), 47-54.

Niaounakis, M., & Halvadakis, C. P. (2006). Olive Processing Waste Management: Literature Review and Patent Survey 2nd Edition (Vol. 5). Elsevier.

Pütün, A. E., Uzun, B. B., Apaydin, E., & Pütün, E. (2005). Bio-oil from olive oil industry wastes: Pyrolysis of olive residue under different conditions. Fuel Processing Technology, 87(1), 25-32.

Roig, A., Cayuela, M. L., & Sánchez-Monedero, M. A. (2006). An overview on olive mill wastes and their valorisation methods. Waste Management, 26(9), 960-969.

Şensöz, S., Demiral, İ., & Gerçel, H. F. (2006). Olive bagasse (Olea europea L.) pyrolysis. Bioresource technology, 97(3), 429-436.

Sharma, A., Pareek, V., & Zhang, D. (2015). Biomass pyrolysis—A review of modelling, process parameters and catalytic studies. Renewable and Sustainable Energy Reviews, 50, 1081-1096.

Snell, R. W., Combs, E., & Shanks, B. H. (2010). Aldol condensations using bio-oil model compounds: the role of acid–base bi-functionality. Topics in catalysis, 53(15-18), 1248-1253.

Taralas, G., & Kontominas, M. G. (2006). Pyrolysis of solid residues commencing from the olive oil food industry for potential hydrogen production. Journal of analytical and applied pyrolysis, 76(1), 109-116.

Uslu, A., Faaij, A. P., & Bergman, P. C. (2008). Pre-treatment technologies, and their effect on international bioenergy supply chain logistics. Techno-economic evaluation of torrefaction, fast pyrolysis and pelletisation. Energy, 33(8), 1206-1223.

Uzun, B. B., Pütün, A. E., & Pütün, E. (2007). Composition of products obtained via fast pyrolysis of olive-oil residue: effect of pyrolysis temperature. Journal of Analytical and Applied Pyrolysis, 79(1), 147-153.

Yin, C. Y. (2011). Prediction of higher heating values of biomass from proximate and ultimate analyses. Fuel, 90(3), 1128-1132.

Zabaniotou, A. A., Kalogiannis, G., Kappas, E., & Karabelas, A. J. (2000). Olive residues (cuttings and kernels) rapid pyrolysis product yields and kinetics. Biomass and bioenergy, 18(5), 411-420.

Zabaniotou, A., Ioannidou, O., Antonakou, E., & Lappas, A. (2008). Experimental study of pyrolysis for potential energy, hydrogen and carbon material production from lignocellulosic biomass. International Journal of Hydrogen Energy, 33(10), 2433-2444.

Zanzi, R., Sjöström, K., & Björnbom, E. (2002). Rapid pyrolysis of agricultural residues at high temperature. Biomass and Bioenergy, 23(5), 357-366.

Wang, D., Xiao, R., Zhang, H., & He, G. (2010). Comparison of catalytic pyrolysis of biomass with MCM-41 and CaO catalysts by using TGA–FTIR analysis. Journal of Analytical and Applied Pyrolysis, 89(2), 171-177.

Zhang, H., Xiao, R., Huang, H., & Xiao, G. (2009). Comparison of non-catalytic and catalytic fast pyrolysis of corncob in a fluidized bed reactor. Bioresource Technology, 100(3), 1428-1434.

Zhang, H., Xiao, R., Jin, B., Xiao, G., & Chen, R. (2013). Biomass catalytic pyrolysis to produce olefins and aromatics with a physically mixed catalyst. Bioresource technology, 140, 256-262.

Zhang, H., Zheng, J., Xiao, R., Jia, Y., Shen, D., Jin, B., & Xiao, G. (2014). Study on Pyrolysis of Pine Sawdust with Solid Base and Acid Mixed Catalysts by Thermogravimetry–Fourier Transform Infrared Spectroscopy and Pyrolysis–Gas Chromatography/Mass Spectrometry. Energy & Fuels, 28(7), 4294-4299.

Tables

Table 1 Elemental analysis of three phase olive wastes

	Olive husk	Olive kernels
C (wt.% d.a.f.)	51.80	49.11
H (wt.% d.a.f.)	6.83	6.16
N (wt.% d.a.f.)	1.32	0.23
O* (wt.% d.a.f.)	40.05	44.50
Ash (wt. %)	1.88	0.48
HHV (MJ kg^{-1})	21.57	20.35
LHV (MJ kg^{-1})	20.07	19.00
Water content (%)	3.66	1.53

d.a.f. - Dry ash free

*Determined by difference

Table 2 Non-catalytic fast pyrolysis mass balances and product properties

	Olive husk			Olive kernels
Pyrolysis Temperature (°C)	450°C	500°C	550°C	500°C
Yield (wt. % db)				
Bio-oil	47.35	37.14	40.15	53.62
Phase	2-phase	2-phase	2-phase	Single
Organics	26.68	18.27	20.26	36.02
Reaction water	20.67	18.87	19.90	17.60
Char	24.69	21.25	21.33	21.02
Gas	14.96	17.90	21.38	16.99
Mass Balance closure	87.00	76.29	82.87	91.63

d.b - Dry basis

d.a.f. - Dry ash free

*Determined by difference

Table 3 Non-catalytic fast pyrolysis - Char analysis results

		Olive husk		Olive kernels
Pyrolysis Temperature (°C)	450°C	500°C	550°C	500°C
Char properties				
Ash (wt.% d.b.)	15.44	14.26	35.10	12.75
C (wt.% d.a.f.)	66.76	61.56	66.70	81.50
H	4.26	3.32	3.40	3.29
N	2.01	1.47	1.63	0.57
O*	26.97	33.65	28.27	14.64
HHV (MJ kg^{-1})	25.08	22.83	24.41	28.25
LHV (MJ kg^{-1})	24.15	22.11	23.67	27.53

d.b - Dry basis

d.a.f. - Dry ash free

*Determined by difference

Table 4 Non-catalytic fast pyrolysis – Bio-oil analysis

			Olive husk				Olive kernels
Pyrolysis Temperature (°C)	450°C		500°C		550°C		500°C
Bio-oil properties							
	Organic	Aqueous	Organic	Aqueous	Organic	Aqueous	Whole
C (wt.% d.a.f.)	52.50	26.82	40.50	25.95	63.91	23.04	45.90
H	8.24	9.40	9.54	9.82	10.44	9.65	7.92
N	1.21	0.70	0.66	0.49	0.88	0.52	0.16
O*	38.05	63.09	49.31	63.75	24.78	66.80	46.03
HHV (MJ kg^{-1})	22.37	15.04	19.31	14.93	26.56	13.93	20.19
LHV (MJ kg^{-1})	20.57	12.99	17.23	12.79	24.29	11.82	18.46
Water content (wt. %)	14.72	50.83	7.06	50.69	10.93	56.69	26.85
pH	4.29	4.60	4.18	4.24	4.82	5.02	4.01
Dynamic Viscosity (cP)	80.8	2.77	111.5	2.73	176	2.19	14.6

d.b - Dry basis

d.a.f. - Dry ash free

*Determined by difference

Table 5 Non-catalytic fast pyrolysis - Chemical composition of the organic fraction (peak area %)

Catalyst	AR	ALI	PH	AC	AL	ALD	KET	PAH	OXY	UN	HV
Olive husk (450°C)	0.0	1.6	27.1	2.8	11.4	2.0	10.8	0.0	1.2	43.1	0.0
Olive husk (500°C)	0.0	1.8	24.4	3.6	10.5	2.5	16.3	0.0	0.9	40.0	0.0
Olive husk (550°C)	0.0	3.3	24.6	5.7	12.8	2.6	20.5	0.0	0.4	30.1	0.0
Olive kernels (500°C)	0.0	0.7	40.0	1.1	5.8	6.6	8.9	0.0	4.6	32.3	0.0

Table 6 Product yield distribution for catalytic experimental runs (wt.% on dry biomass)

Catalyst	Liquid Yield	Gas Yield	Solid Yield	H_2O yield	Organic yield
Silica sand	52.66	19.11	28.23	21.67	30.99
ZSM-5	47.03	23.71	29.26	27.34	19.68
MgO	46.72	23.47	29.82	25.57	21.15
ZSM-5(5% Co)	48.51	23.87	27.63	32.17	16.34
MgO(5% Co)	43.96	23.23	32.81	23.71	20.25

Table 7 Gas product yields for catalytic experimental runs (wt.% on biomass)

Catalyst	CO_2	CO	H_2	CH_4	C_2	$C_2=$	C_3	$C_3=$	C_4-C_6	Gas Yield
Silica sand	12.80	4.11	0.03	0.78	0.28	0.22	0.11	0.19	0.60	19.11
ZSM-5	13.52	5.80	0.03	0.80	0.28	0.56	0.11	0.87	1.75	23.71
MgO	15.68	4.64	0.04	1.05	0.41	0.31	0.19	0.30	0.86	23.47
ZSM-5(5% Co)	14.35	5.28	0.05	0.91	0.26	0.65	0.12	0.96	1.29	23.87
MgO(5% Co)	15.79	4.37	0.18	0.88	0.33	0.26	0.16	0.27	0.99	23.23

Table 8 Catalytic pyrolysis - Chemical composition of the organic fraction (peak area %)

Catalyst	AR	ALI	PH	AC	AL	ALD	KET	PAH	OXY	UN	HV
Silica sand	0.0	0.0	2.9	21.1	0.0	0.0	0.0	0.0	2.3	42.2	31.5
ZSM-5	11.9	0.9	32.3	4.0	0.3	0.0	2.8	2.1	3.3	42.4	0.0
MgO	1.2	10.3	16.0	10.5	2.5	0.0	3.6	0.5	7.0	48.4	0.0
932F/100cc/ZSM-5(5% Co)	3.5	0.4	25.7	11.4	1.2	1.1	1.8	2.3	2.6	35.8	14.2
932F/100cc/MgO(5% Co)	1.2	1.9	13.4	15.1	5.0	0.7	5.5	0.6	4.1	27.9	24.7

Table 9 Elemental composition of the produced bio-oils (wt.% on dry organic fraction).

Catalyst	Carbon	Hydrogen	Oxygen*
Silica sand	53.98	8.95	37.06
ZSM-5	63.16	10.04	26.80
MgO	63.78	12.29	23.93
ZSM-5(5% Co)	67.75	6.42	25.83
MgO(5% Co)	60.63	9.57	29.80

*Determined by difference

Figure Captions

Figure 1: Fluidized bed fast pyrolysis rig

Figure 2: Experimental set-up for catalytic pyrolysis

Figure 3: Non-catalytic fast pyrolysis gases

Figure 4: Non-catalytic fast pyrolysis – Bio-oil GC/MS chromatograms: (a) OH-500, (b) OH-550, (c) OH-450, (d) OK-500

Figures
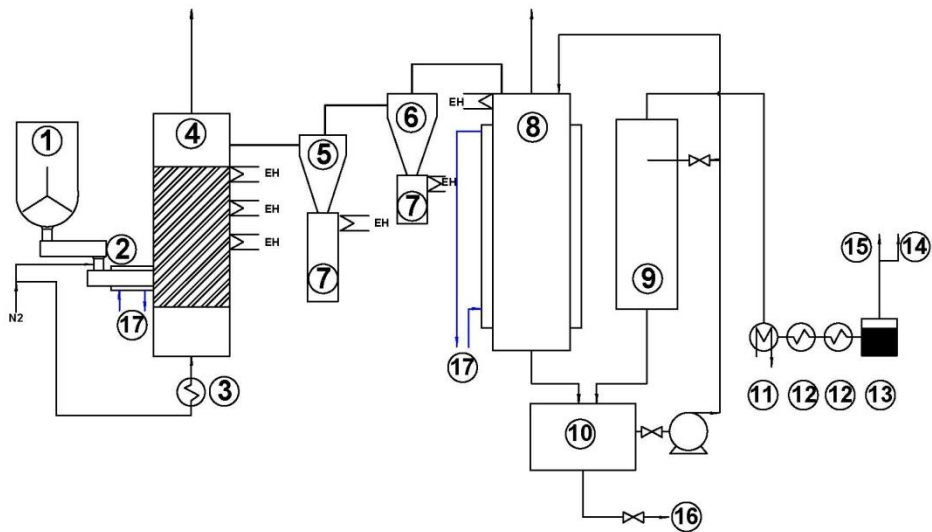
1- feed hopper, 2-screw, 3- N2 pre- heater, 4- BFB reactor, 5- cyclone 1, 6- cyclone 2, 7- char pot, 8- quench column, 9- electrostatic precipitator, 10- collection tank, 11 - water cooled condenser, 12- dry-acetone condenser, 13-cotton wool filter, 14 - to Micro GC, 15- gas vent, 16- bio-oil, 17 - cooling water
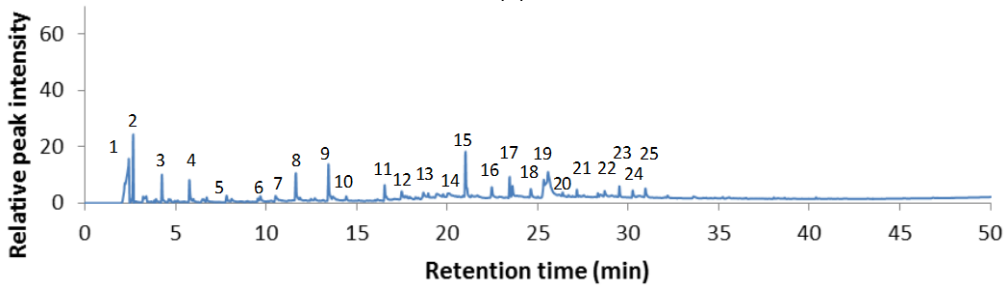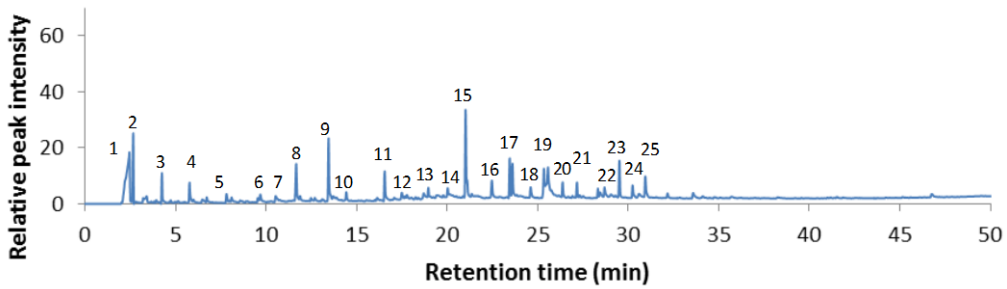
Figure 1
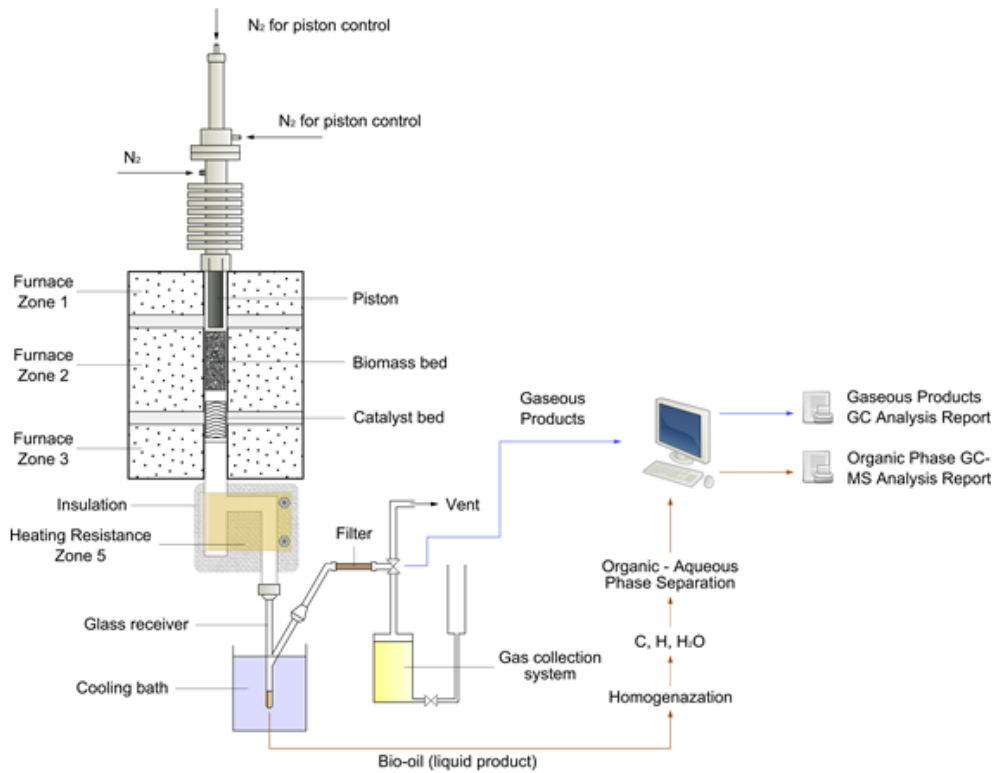
Figure 2

Figure 3

(a)

(b)

(c)

(d)

Figure 4